EXPERIMENTAL DESIGN

Instrumentation, consisting of a 3 frequency acoustic backscatter sensor (ABS) (Pearson and Thomas, 1990) and a Valeport 3.2 cm diameter discuss head electromagnetic current meter (EMCM) were mounted on an H-frame at approximately the mid-tide position (Figure 3). Additional instrumentation consisting of electromagnetic current meters, optical backscatterance sensors, pressure sensors and mechanical syringe samplers were also deployed, however, in this paper the analysis has been restricted to the bed position information from the ABS and nearbed current information from the 3.2 cm diameter discuss head EMCM.

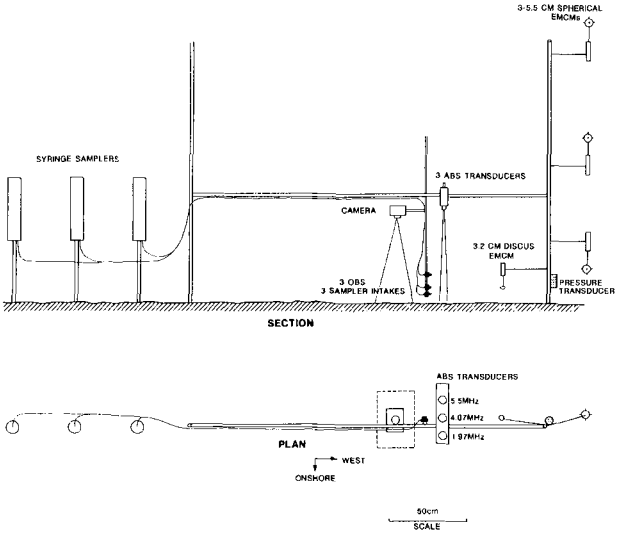

Figure 3. Schematic of the instrumented H-frame.

Local bed elevations were measured with a vertical resolution of 5 mm at 3 horizontal positions approximately 0.10 m apart on a cross-shore transect using the 3 ABS transducers. SCUBA divers also made measurements of the bed profile beneath the ABS transducers by means of a bedform measurement device (Osborne and Vincent, in prep) and took detailed notes on the bedform geometry, bedform migration and suspension characteristics throughout the high-speed data collection runs. Although an underwater camera was mounted adjacent to the ABS, no information on ripple migration could be obtained due to lack of visibility.

The sensors were shore-connected and the data were recorded on a single PC-based data logging system. In order to satisfy the aims and objectives of the BASEX program there was a need for two separate approaches to computerized data collection within the same experimental design. In order to resolve the kinematics of the re-suspension process relative to wave motions and small scale ripple patterns

it was necessary to sample as rapidly as possible to achieve a high spatial and temporal resolution and also to keep runs short enough such that the bed topography did not change significantly relative to the sensors. In order to resolve the effects of different hydrodynamic conditions on bed response it was necessary to collect data over longer periods, more or less continuously, and over a number of tidal cycles. Therefore, two sampling modes were adopted for data collection during this deployment:

1. **Rapid sampling mode** produced short duration data collection runs with relatively high temporal resolution. In this case 12 acoustic profiles initially sampled at 150 kHz were collected from each transducer and averaged to one profile per transducer. The data between 0.10 - 0.65 m range at 0.005 m intervals were stored together with a single digitised value from the EMCM channels. This scheme resulted in an overall collection rate of 4.22 Hz. Available storage space allowed the collection of 1050 profiles for a run duration of 250 s.

2. In **slow sampling mode** run durations were increased to as much as 30 minutes by averaging over a larger number of acoustic profiles (24-48) and storing a smaller vertical range (0.53-0.67 m) of the acoustic data. This scheme resulted in a slower overall collection rate of 1.1-2.1 Hz but enabled continuous observation of bed elevation changes over periods of 30 minutes.

Measurements were made during daylight hours over half tidal cycles from high water down to low water or from low water up to high water.

ACOUSTIC MEASUREMENTS OF SEA BED POSITION

ABS detect the presence of the bottom boundary due to the change in material density between the fluid and bed which cause a strong acoustic reflection (Hanes et al., 1988). The position of the sea-bed is defined as the position of maximum recorded acoustic pressure. In most acoustic profiles of the water column, the bottom location is clearly identified by a sharp peak in the backscattered pressure. It is therefore relatively simple to produce an algorithm which detects the maximum acoustic return from each profile in order to produce a time-series of bed positions (Figure 4).

Sampling the backscattered acoustic signal at a rate of 150 kHz and range-gating enabled the determination of bed position to +/- 0.005 m under ideal conditions. Clearly, there are random instantaneous variations in the maximum acoustic return above and below the true bed position in Figure 4 which reduce the degree of certainty about the actual bed position at any instant in time. However, these short-term deviations, which may be due to a combination of signal attenuation by suspended sediment and bubbles, and multiple echoes, may be removed relatively easily by a combination of de-spiking and smoothing. More importantly, there are

also significant temporal trends which occur in the data. These variations in the series are interpreted as real changes in the bed position. The series in Figure 4 suggests that 3-4 cm of erosion occurred over a period of 6 minutes followed by 2-3 cm of accretion in the next 6 minutes.

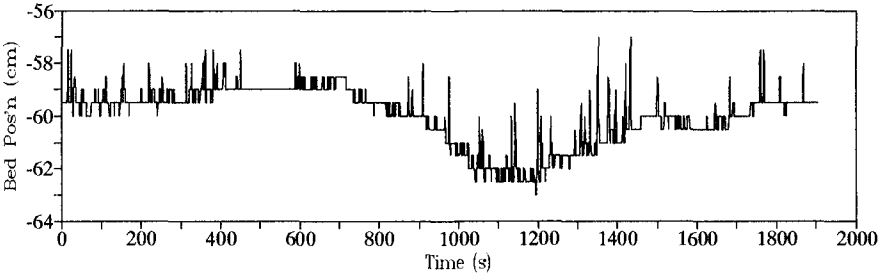

Figure 4. Time-series of the position of maximum backscattered pressure after smoothing by Hanning 3 times. Resolution of the ABS is 5 mm.

CHANGES IN SEA BED POSITION DURING A TIDAL CYCLE

Time series of bed positions were reduced to one representative value of bed position for each two minute segment of a data run. A series of reduced bed positions from one transducer, representative of a falling portion of a tidal cycle is shown in Figure 5 c. Burst-averaged zero-crossing periods of the cross-shore flow, water depths, cross-shore and shore-parallel velocities, and significant range of cross-shore flows associated with these bed positions are shown in Fig. 5 a and b. The two lines in the bed position series indicate the uncertainty in measured bed position due to sampling resolution (+/- 1 bin) of the ABS. The first 30 minutes of the series shows variations in bed position of no more than 2 cm. Over the next 30 minutes, there is an accretion of 2.5 cm followed by erosion of 6 cm. During the final 15-20 minutes of the series there is a rapid accretion of 8 cm.

In general, the high tide periods (depths 1.5-2.0 m in this experiment) were characterized by near-bed wave-orbital speeds of less than 0.75 m s^{-1} and relatively small and gradual changes in vertical bed position (usually < 0.5 cm min^{-1}) (Figure 6). In contrast, under rapidly rising and falling water levels (depths of 0.5-1.5 m in this experiment), particularly as waves are forced to shoal and break, wave orbital speeds were greater than 0.75 m s^{-1} and bed position changes were often substantially larger and more rapid (upto 1.0 cm min^{-1}).

BED PROFILE RECONSTRUCTION AND BEDFORM MIGRATION

Although the 3 ABS transducers were mounted in fixed positions it is possible to use bed position information together with the detailed diver measurements of the bed beneath the transducers to reconstruct bed profiles and calculate bedform migration rates. A time sequence of bed profiles has been reconstructed (Figure 7) from the ABS bed position measurements (Figure 5) and SCUBA diver observations during the falling tide. The sequence began with small symmetric, two-dimensional vortex ripples (height = 2.5 cm and spacing = 10 cm) and ended with large asymmetric landward lunate megaripples (height = 8 cm and spacing = 40-50 cm). This increase in both height and spacing with time is clearly visible in the profiles. The profiles between 40-65 minutes also indicate shoreward migration of the bedform at a rate of approximately 2.0 cm min^{-1}.

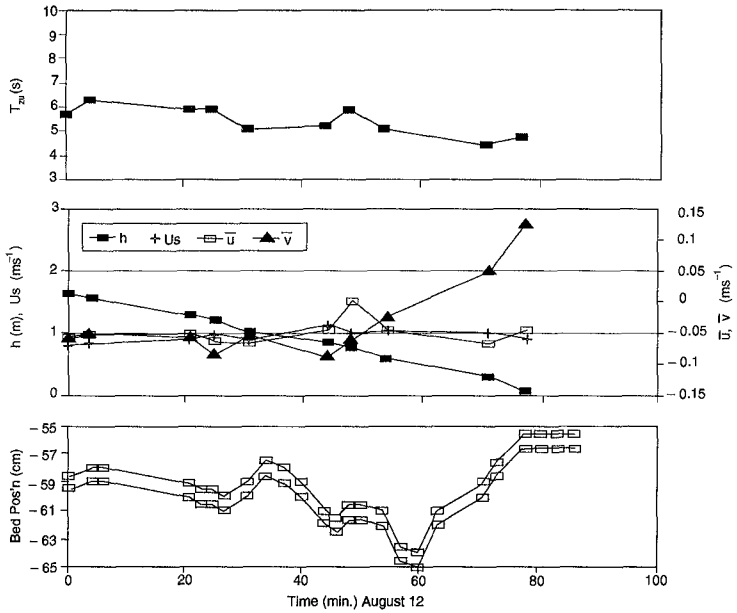

Figure 5. Series of burst-averaged zero crossing periods of the cross-shore flow, T_{zu}, (a); water depths, h, cross-shore flows, u, shore-parallel flows, v, significant cross-shore velocity ranges, U_s, (b); and reduced bed positions (c), representative of falling portion of a spring tide.

DISCUSSION AND CONCLUSIONS

Large and rapid changes in bed elevation were observed during spring tidal cycles under low energy swell conditions with little or no mean currents present. The largest changes in bed elevation are associated with smaller depths when wave induced cross-shore flows are large and waves are either breaking or near breaking. Changes were associated with bedform development resulting from changes in the local hydrodynamic forcing as well as with bedform migration. These processes accounted for local bed elevation changes of upto 10 cm during a series of tidal cycles in which no significant local net erosion or accretion took place.

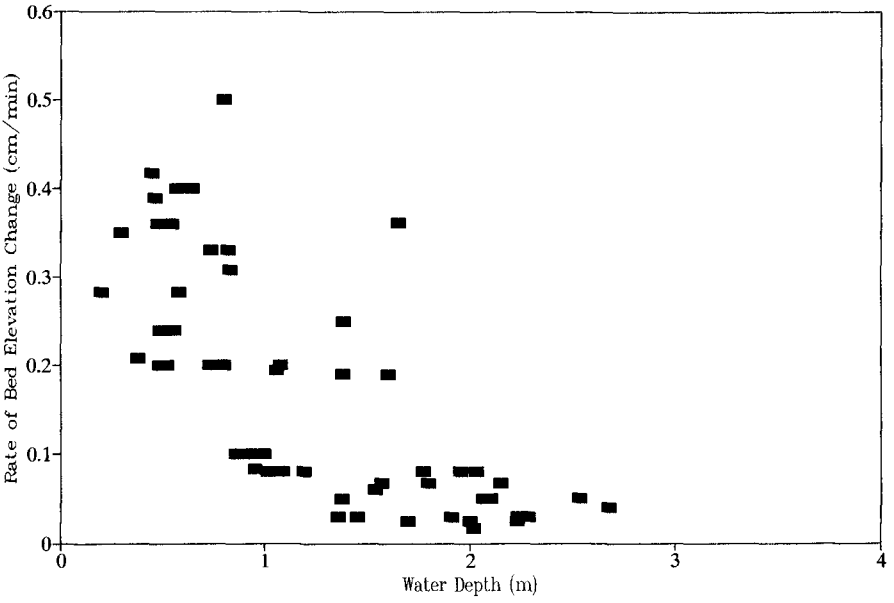

Figure 6. Variations in the time-averaged rate of vertical bed position change as a function of water depth.

Bedform migration rates of upto 2.2 cm min^{-1} were associated with well-defined lunate mega-ripples (height = 8 cm; wavelength = 40 cm) under spilling and shoaling waves. Excluding sediment by-passing this represents a total load transport rate of approximately 0.7 gm cm^{-1} s^{-1}. Evidently, form migration under these conditions represents a significant contribution to the net sediment transport. Bedform migration rates were 1 cm min^{-1} and less under the lower energy conditions associated with greater water depths at high tide. The observed bedform migration rates suggest that local bed elevation changes of upto 1.0 cm min^{-1} can be expected under large-scale migrating lunate mega-ripples, while rates of bed elevation change upto 0.6 cm min^{-1} can be expected under the small-scale three-dimensional and two-dimensional vortex type forms.

These findings have significant implications for measurement and interpretation of sediment transport rates in wave and current environments. As an example, Figure 8 shows time-series of de-spiked and smoothed bed position, suspended sediment concentrations at 2 cm above an arbitrary fixed bed position (indicated by the dashed line in Figure 8 a), suspended sediment concentrations at 2 cm above the measured time-varying bed position, and cross-shore velocity. The uncompensated concentration series (Figure 8 b) is representative of the type of measurements which would be obtained by a fixed point sensor such as an optical backscatterance sensor or transmissometer. There is clearly a non-stationary trend in this series which is coherent with the rising bed position. The trend is absent from the series compensated for bed position change (Figure 8 c). Interpretation of sediment re-suspension processes and computations of sediment transport rates from point measurements of sediment concentration and velocity will be subject to potentially large errors without compensation for bed position changes relative to instrument positions when large and rapid bed elevation changes occur. In the example shown, the time-integrated cross products between velocity and concentration differed by 30 % for the compensated as opposed to uncompensated series. Furthermore, the presence of migrating large-scale bedforms under relatively gentle conditions suggests that spatial variability in sediment concentrations, near-bed velocity structure and sediment transport are likely to be significant.

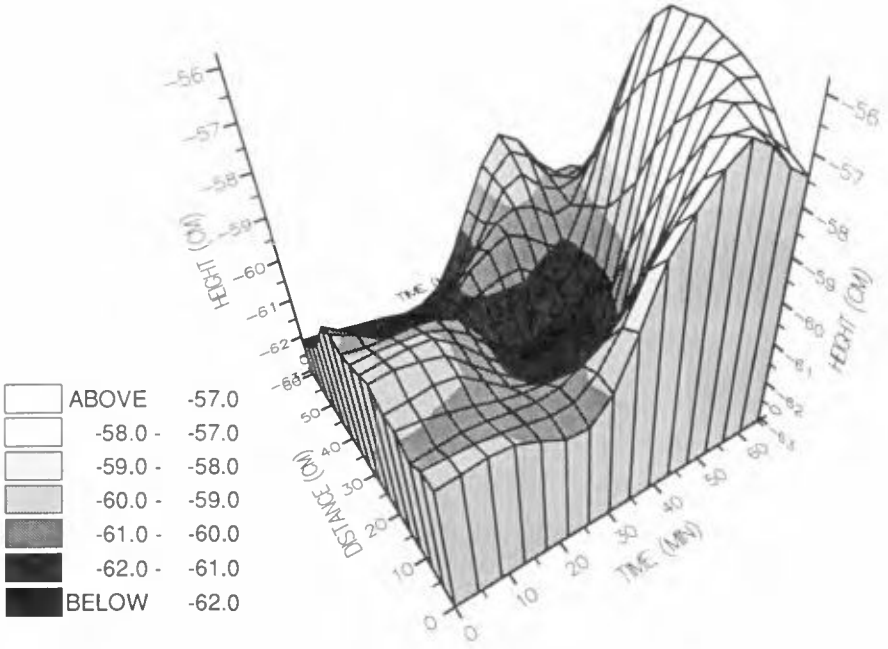

Figure 7. Time-sequence of reconstructed bed profiles during a falling tide.

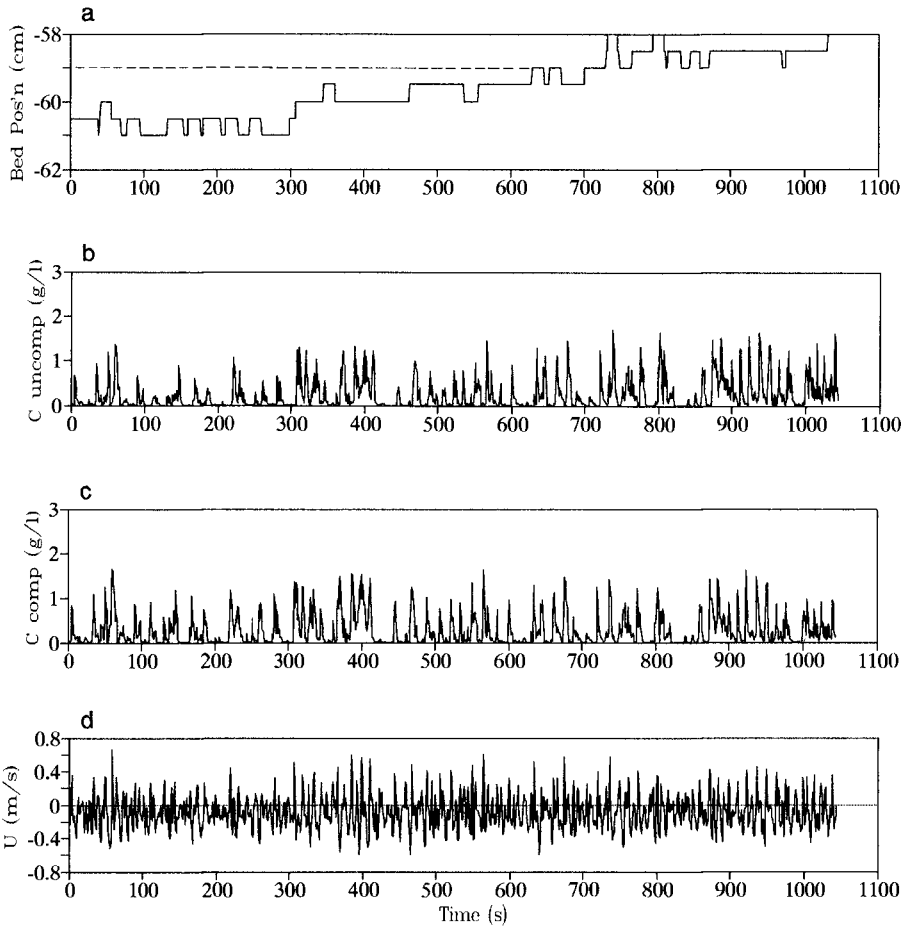

Figure 8. Time-series of: a) smoothed and de-spiked bed position; b) suspended sediment concentration at 2 cm above fixed bed (dashed line in a); c) suspended sediment concentration at 2 cm above true bed position; d) cross-shore velocity.

ACKNOWLEDGEMENTS

The BASEX programme is a combined project involving the University of East Anglia, Bullard Laboratories, and the University of Plymouth. BASEX is sponsored by the Natural Environment Research Council. PDO also gratefully acknowledges the support of a Natural Sciences and Engineering Research Council of Canada Postdoctoral Fellowship. The authors wish to thank Drs. Malcolm Green, Mark Davidson, Paul Russell and Mr. Gareth Lloyd for their enthusiastic assistance while in the field. Particular thanks to Professor David Huntley for making the B-Band instrumentation available and for arranging access to the beach.

REFERENCES

Dingler, J.R. (1974) Wave-formed ripples in nearshore sands. Ph.D. Dissertation, Univ. of California, San Diego, 136 pp.

Dingler, J.R., Boylls, J.C. and Lowe, R.L (1977) A high-frequency sonar for profiling small-scale subaqueous bedforms. Marine Geology, 24: 279-288.

Greenwood, B., Dingler, J.R., Sherman, D.J., and Anima, R.J. (1984) Bedform dynamics and bedding genesis under waves, Pointe Sapin, New Brunswick: I Design, construction and testing of a high resolution remote tracking sonar (HRRTS). Canadian Coastal Sediment Study C2S2-7, National Research Council of Canada, Associate Committee for Research on Shoreline Erosion and Sedimentation, Ottawa, pp. 75-91.

Hanes, D.M., Vincent, C.E., Huntley, D.A. and Clarke, T.L. (1988) Acoustic measurements of suspended sand concentration in a wave-dominated nearshore environment. Continental Shelf Research, 6 (4): 585-596.

Osborne, P.D. and Vincent, C.E. (in preparation) Bedform dynamics on a macro tidal beach.

Pearson, N.D. and Thomas, M.R. (1990) A multi-frequency acoustic backscatter recorder for suspended sediment transport studies. Proc. Inst. Elec. Eng. Colloquium Monitoring the Sea, Digest no. 1990/182.

Vincent, C.E. and Green, M.O. (1990) Field measurements of the suspended sand concentration profiles and fluxes, and of the resuspension coefficient over a rippled bed. J. Geophys. Res., 95: 15591-15601.

Vincent, C.E., Hanes, D.M. and Bowen, A.J. (1991) Acoustic measurements of suspended sand on the shoreface and the control of concentration by bed roughness. Marine Geology. 96: 1-18.

CHAPTER 179

SHORELINE CHANGE AT OREGON INLET TERMINAL GROIN

M. F. Overton (M)[1], J. S. Fisher (M)[2]
W. A. Dennis (M)[3], and H. C. Miller (AM)[4]

Abstract

The Oregon Inlet Terminal Groin was completed in 1991. The groin was built to provide protection to the bridge crossing the inlet. A detailed monitoring program has analyzed shoreline position with the use of aerial photographs collected every two months. To date, no adverse impacts of the groin have been found on the shoreline within a 6 mile distance downdrift of the groin.

Introduction

Oregon Inlet is located between Bodie Island and Pea Island on the North Carolina coast, Figure 1. These islands form a part of the barrier island system generally referred to as the Outer Banks. This inlet formed in 1846 during a major storm, and has remained open to the present. During this 146 year interval the inlet has gone through many changes in width and position, with a net migration to the south of approximately 2 miles. The inlet width has varied from a minimum of about 2,000 ft to a maximum of just over 5,000 ft. While there have been numerous discussions and plans to stabilize it with jetties, Oregon Inlet remains one of the largest unimproved inlets along the east coast of the United States.

The inlet is spanned by the 2.4 mile long Bonner Bridge constructed in 1962, Figure 2. This bridge is located along the

[1]Dept. Civil Engineering, NCSU, Raleigh, NC 27695-7908
[2]Dept. Civil Engineering, NCSU, Raleigh, NC 27695-7908
[3]US Army COE, Wilmington District, P.O. Box 1890, Wilmington, NC 28502
[4]US Army COE, FRF, 1261 Duck Rd., Kitty Hawk, NC 27949

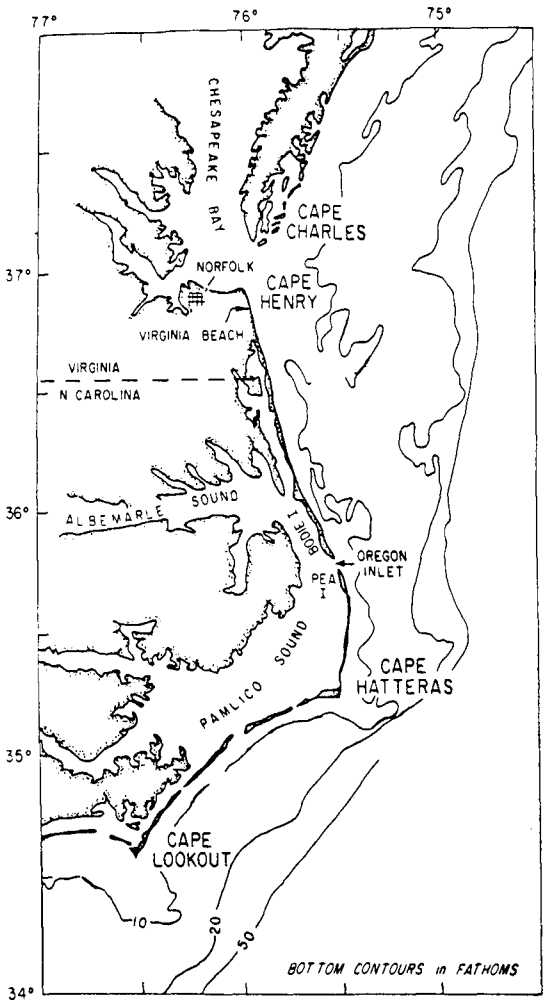

Figure 1. Location of Study Area
(from Inman and Dolan, 1989)